Metabolomic profiling and comparison of major cinnamon species using UHPLC–HRMS

Yifei Wang[1,2], **Peter de B. Harrington**[2], **Pei Chen**[1,*]

[1]Methods and Application of Food Composition Laboratory, U.S. Department of Agriculture, Agricultural Research Service, Beltsville Human Nutrition Research Center, Beltsville, MD 20705, USA

[2]Department of Chemistry & Biochemistry, College of Arts and Sciences, Ohio University, Athens, OH 45701, USA

Abstract

The metabolomic profiles of four major species of cinnamon (*Cinnamomum verum*, *C. burmannii*, *C. loureiroi*, and *C. cassia*) were investigated by ultra-high-performance liquid chromatography – high-resolution mass spectrometry (UHPLC–HRMS). Thirty-six metabolites were tentatively characterized, belonging to various compound groups such as phenolic glycosides, flavan-3-ols, phenolic acids, terpenes, alkaloids, and aldehydes. Principal component analysis (PCA) and partial least squares - discriminant analysis (PLS-DA) on the HRMS data matrix resulted in a clear separation of the four cinnamon species. Coumarin, cinnamaldehyde, methoxycinnamaldehyde, cinnamoyl-methoxyphenyl acetate, proanthocyanidins, and other components varied among the four species. Such variations were used to develop a step-by-step strategy for differentiating the four cinnamon species based on their levels of pre-selected components. This study suggests a significant variation in the phytochemical compositions of different cinnamon species, which have a direct influence on cinnamon's health benefit potentials.

Graphical Abstract

*Corresponding Author: pei.chen@usda.gov.

Conflicts of interest/Competing interests: The authors declare that they have no conflict of interest.

Availability of data and material: Datasets and materials generated or analyzed during the current study are available from the corresponding author upon reasonable request.
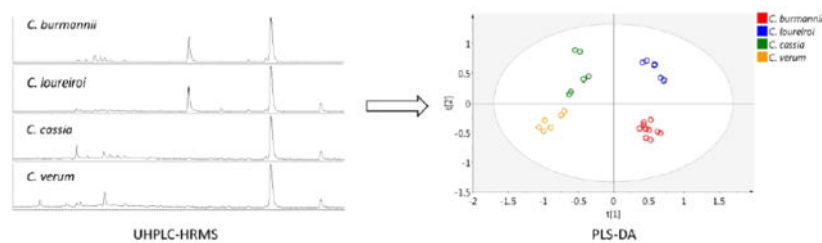
Introduction

Cinnamon is a spice that has been commonly used around the world for centuries [1]. It is produced from the dried inner bark of several evergreen tree species belonging to the genus *Cinnamomum* of the Lauraceae family. Four *Cinnamomum* species are economically important as widely used spices and were traditionally named by their primary growth regions, including *C. verum* ("true cinnamon", also called Ceylon or Sri Lankan cinnamon), *C. burmannii* (Korintje or Indonesian cinnamon), *C. loureiroi* (Saigon or Vietnamese cinnamon), and *C. cassia* (Chinese cinnamon) [2]. Besides these four species, there are many other less common cinnamon varieties that are used as local spices or herbal medicine ingredients, such as *C. tamala* (Indian cassia) and *C. citriodorum* (Malabar cinnamon) [3].

In addition to its culinary uses, the medicinal values of cinnamon also have been employed by different cultures. The use of cinnamon as herbal medicine was recorded in Chinese literature over 4000 years ago [4, 5]. In traditional Ayurvedic medicine, cinnamon has been used for treatment of diarrhea, arthritis, and menstrual irregularities [6]. Many countries are still using cinnamon as a carminative and stomachic for gastrointestinal disorders [1]. Modern studies utilizing different *in vitro* or *in vivo* models have reported various cinnamon health-promoting activities, such as anti-inflammatory, antioxidant, antimicrobial, and anti-cancer properties, cardiovascular benefits, and regulation of glucose and lipid metabolism [1, 2, 7-9].

The emerging evidence of cinnamon's beneficial pharmacological effects have led to growing research interest of its phytochemical profile. Cinnamon contains high levels of essential oils, with cinnamaldehyde as the major component which gives cinnamon its characteristic odor and flavor [1]. Other determined cinnamon components consist of phenolics, terpenoids, saponins, and phytosterols [10-14]. Many of these compounds have been shown to directly contribute to cinnamon's various bioactivities. For instance, cinnamaldehyde and proanthocyanidins were determined as major active components for cinnamon's antibacterial properties [7]. Cinnamaldehyde was also identified to primarily contribute to cinnamon's anti-neuroinflammatory effect [15]. Several cinnamon phenolics were characterized to have strong inhibitory activity against tyrosinase [16]. A-type proanthocyanidins were found to possess insulin-like bioactivity and provide cinnamon's antidiabetic properties [11].

Different cinnamon species have varied chemical compositions. Most notable is coumarin, which occurs at higher concentrations in three of the four major species except for *C. verum* [17]. On the other hand, *C. verum* has a higher ratio (~95%) of cinnamaldehyde in its essential oils compared to *C. cassia* (40-65%), while the latter contains cinnamic acid and cinnamyl alcohol as additional components [1, 18]. Based on such observations, an authentication method was developed to differentiate *C. verum* samples from other species using direct analysis in real-time (DART)-quadrupole ion trap time-of-flight (QToF)-mass spectrometry (MS) and multivariate analysis [19]. Similarly, in our group's previous study, four major cinnamon species were successfully differentiated by their chemical fingerprints acquired from flow injection mass spectrometry (FIMS) [20]. These findings further illustrated the variations of the different cinnamon species' chemical compositions.

Analyses of certain cinnamon components have been also adopted in different cinnamon monographs, such as their identities, purities, and contaminants. Compared to the aforementioned full-scale chemometric analyses using fingerprints acquired from authentic materials, sample identification using monographs targets pre-selected components to identify samples without the need of multiple authentic reference materials which can be difficult to obtain for many labs. The United States Pharmacopeia (USP) has proposed several monographs for cinnamon materials such as the bark or twig of *C. cassia* and *C. verum* [21]. While standard test methods were provided in these monographs for sample identification, their abilities of differentiating one cinnamon species from the others are rather limited. A monograph-style approach on differentiating major cinnamon species based on pre-selected components and rules will be of great value.

The health benefit potential has become one of the most important aspects in cinnamon quality evaluation, and is directly related to the chemical profiles of each species. Although previous studies have reported significant variation of certain cinnamon components, there is a lack of analyses on full-scale profiling and comparison of phytochemicals in different cinnamon species. In the current study, cinnamon samples obtained from the four major species - *C. verum*, *C. burmannii*, *C. loureiroi*, and *C. cassia* were analyzed by ultra-high-performance liquid chromatography – high-resolution mass spectrometry (UHPLC–HRMS). Major and minor cinnamon components were characterized to provide detailed knowledge on their chemical composition. In addition, multivariate analyses were used to perform nontargeted metabolomic comparisons on the different cinnamon species and identify components that varied significantly. An identification strategy using LC/MS data of selected cinnamon components was proposed to accurately differentiate the four species without authentic materials.

Materials and Methods

1. Cinnamon materials and reagents

Fourteen cinnamon products in forms of powder, chip or stick were purchased online and labelled as CM-1 to CM-14. Based on the product label (name and/or origin), they were obtained from the four major *Cinnamomum* species - *C. verum*, *C. burmannii*, *C. loureiroi*, and *C. cassia*. List of these cinnamon products is given in Table 1. Cinnamon samples were

further analyzed by DNA barcoding (NSF AuthenTechnologies, Petaluma, CA) to verify their identities and determine potential contaminants/adulterants.

Methanol, acetonitrile, and formic acid were purchased from Fisher Scientific (Pittsburg, PA) and were in Optima® LC/MS grade. Ultrapure water was produced from a Barnstead™ Nanopure™ water purification system (Thermo Scientific, Waltham, MA). Trans-cinnamic acid and (-)-epicatechin were obtained from Sigma-Aldrich (St. Louis, MO).

2. Sample preparation and extraction

Cinnamon samples in non-powder forms were first ground into fine powders by a Retsch® RM100 mortar grinder (Retsch GmbH & Co. KG, Haan, Germany). Cinnamon powders (50 mg) were weighed into 15 mL centrifuge tubes and extracted by 5 mL 60% methanol through 20 min of sonication at room temperature and 10 min of centrifugation at 5,000 g. Supernatants were collected and filtered through 0.2 μm PVDF syringe filter (Thermo Scientific, Waltham, MA) prior to UHPLC–HRMS analysis.

3. UHPLC–HRMS apparatus and conditions

The UHPLC–HRMS analysis was conducted in a Thermo Scientific Vanquish Horizon UHPLC system (binary pump, autosampler, column compartment, and PDA detector) coupled with a Thermo Scientific Orbitrap ID-X tribrid mass spectrometer (Thermo Scientific, Waltham, MA). A Hypersil GOLD aQ column (200 × 2.1 mm, 1.9 μm particle size) (Thermo Scientific, Waltham, MA) was used for the LC separation. A binary solvent system was used with solvent A as 0.1% formic acid in water and solvent B as 0.1% formic acid in acetonitrile. The elution gradient was 2% B between 0 - 5 min; 2% - 35% B between 5 - 30 min; 35% - 55% B between 30 - 40 min; 55% - 95% B between 40 - 42 min and 95% B between 42 - 52 min with flow rate at 0.25 mL/min. The column was heated at 50 °C and equilibrated with 2% B for 10 min between injections. The injection volume was 2 μL.

HRMS data was acquired in fast chromatography MS2 mode, using the following parameters: ion source: H-ESI, positive ion; spray voltage: 3.5 kV; sheath gas: 50 Arb; aux gas: 10 Arb; sweep gas: 2 Arb; ion transfer tube temperature: 325 °C; vaporizer temperature: 350 °C. For master MS scan, the following parameters were applied: detector type: orbitrap; orbitrap resolution: 50,000; scan range: m/z 100-2000. Both intensity threshold (1.0×10^4) and dynamic exclusion (exclude after 1 time for 2.5 s) filters were applied for data-dependent MS2 scan, which was conducted under the following parameters: isolation mode: quadrupole; activation type: HCD; HCD collision energies: stepped, 10,15,25; detector type: orbitrap; orbitrap resolution: 30000; first mass: m/z 50. Data were acquired and processed in Xcalibur™ 4.2 (Thermo Scientific, Watham, MA). Two repeated analyses of 14 samples resulted in a total of 28 acquisitions.

4. MS data processing for multivariate analysis

MS data of 28 acquisitions were exported into Progenesis QI software (Nonlinear Dynamics, Newcastle, UK) for automatic ion deconvolution, peak selection, and peak alignment. Data within the retention time range between 3 and 40 min were selected for analysis. A total of 1137 unique ions were detected across all samples and were exported into a two-

dimensional 28×1137 (samples × mass peaks) matrix in Excel. Each mass peak in the matrix was associated with retention time and high-resolution *m/z* data.

5. Statistical analysis

The MS data matrix generated from Progenesis QI was imported into SIMCA software (version 14, Umetrics, Umeå, Sweden) for both principal component analysis (PCA) and partial least squares - discriminant analysis (PLS-DA). Data were normalized to unit vector length, mean-centered, and Pareto scaled (i.e., scaled by the square root of the standard deviation) prior to the analyses. Plots of PCA and PLS-DA scores were acquired to visualize sample clustering and separation. Variable loadings in PCA and their variable importance in projection (VIP) scores in PLS-DA were determined to identify important metabolites contributing to the sample separation. A second MS data set containing only determined important metabolites was extracted from the original.

The support vector tree classifier (SVMTreeH) was constructed using the two MS data sets described above in MATLAB (MathWorks, Natick, MA) [22]. Bootstrapped Latin partition (BLP) was used to unbiasedly evaluate the classifier [23, 24]. The training and experiment sets were selected using 2 Latin partitions that were bootstrapped for 100 times. The classification results from all partitions were pooled and averaged across the 100 bootstraps. Average prediction accuracies between the two data sets were compared.

To compare the ion abundance values of cinnamon metabolites among different species, one-way ANOVA with post-hoc Tukey HSD tests were conducted using SPSS Statistics (version 19, IBM, Armonk, NY).

Results and Discussion

1. DNA authentication of cinnamon samples

Prior to UHPLC–HRMS analysis, the 14 cinnamon products were first analyzed by DNA barcoding to verify their purported identities. Product details and DNA barcoding results are summarized in Table 1. Due to the limitation of the reference DNA sequence database, two cinnamon species - *C. loureiroi* and *C. cassia* could not be differentiated from each other. The assignment of cinnamon samples into these two species was based on sample labeling which indicates their origins. The DNA authentication results of most samples were consistent with their product information. However, some inconsistencies were discovered. Specifically, CM-4, which was ambiguously labelled as both "Cassia" and "Korintje", was identified as *C. burmannii*. CM-5 which was labelled as "Organic Korintje cinnamon" (*C. burmannii*) and had Indonesian origin, contained more DNA sequences of *C. loureiroi* or *C. cassia* than those of *C. burmannii*. Based on the sample labeling and DNA authentication results, the 14 cinnamons were assigned into the following species: CM-1 to CM-4 - *C. burmannii*; CM-6 to CM-8 - *C. loureiroi*; CM-9 to CM-11 - *C. cassia*; CM-12 to CM-14 - *C. verum*. CM-5 could contain multiple cinnamon species including *C. burmannii*, *C. loureiroi*, and *C. cassia*. In summary, although DNA barcoding worked in cases, the limitation of reference sequence database and ambiguous results on certain samples suggest that DNA barcoding cannot be relied on for satisfactory cinnamon species authentication.

2. Identification of cinnamon metabolites among different species

The representative MS chromatograms of the 4 cinnamon species are given in Fig. 1. The ions were putatively identified by comparing their accurate mass and fragmentation data, UV-Vis spectra, and retention times with authentic standards, previous publications, or available databases. Table 2 summarizes the LC-MS data and identities of the characterized cinnamon metabolites. Different identification confidence levels are associated with HRMS analysis [25]. Except epicatechin (peak 14) and trans-cinnamic acid (peak 33), which structures were confirmed by authentic standards (level 1 confidence – confirmed structure), putative identifications (level 3 confidence – tentative candidate) were carried out to other metabolites based on their molecular and fragment ion data.

Peaks 31, 35, and 36 have noticeably high intensities among the different samples and are major cinnamon components. Peak 35 being the most dominant peak across all the samples had its [M+H]$^+$ ion at m/z 133.0646, suggesting the formula of C_9H_8O (−0.19 ppm). With fragment ions at m/z 55, 105, and 115, it was identified as cinnamaldehyde. This compound is the most abundant component in cinnamon essential oil and is responsible for the spice's characteristic aroma and flavor [1]. Peak 36 has a [M+H]$^+$ ion at m/z 163.0755 ($C_{10}H_{10}O_2$, 0.14 ppm) and the major fragment ion at m/z 55 identified it as methoxycinnamaldehyde, which has been reported as a major essential oil component in *C. verum* and *C. cassia* [9]. Peak 31 has a [M+H]$^+$ ion at m/z 147.0439 ($C_9H_6O_2$, −0.16 ppm) and its main fragment ion at m/z 103. The neutral loss of 44 Da suggests the COO moiety in its structure and it was identified as coumarin, another reported major cinnamon constituent [17].

Seventeen peaks, including peaks 2, 4, 5, 7-11, 14, 15, 19-21, 23, 24, 26, and 29, were identified as A-type or B-type proanthocyanidin (PAC) monomer and oligomers. The peaks have the PAC characteristic UV spectral features with a 278-280 nm maximum absorbance [26, 27]. Peak 14 has a [M+H]$^+$ ion at m/z 291.0866 ($C_{15}H_{14}O_6$, −0.22 ppm) and is identified as epicatechin after comparing its retention time and MS fragments with the reference standard. Peaks 4, 5, 10, and 29 with the same molecular formula of $C_{30}H_{26}O_{12}$ were identified as B-type PAC dimers (DP-2, DP as degree-of-polymerization). The B-type PAC dimers shared a strong fragment at m/z 291, which corresponds to the ion of a monomer fragment. Similarly, peaks 19, 21, 23, and 26 were identified as B-type PAC trimers to pentamers based on their molecular (m/z = 867, 1155, or 1443) and fragment ions. Other peaks were identified as A-type PAC trimers (peaks 15 and 20; m/z = 865), tetramers (peaks 2, 7, 11, and 24; m/z = 1153), or pentamers (peaks 8 and 9; m/z = 1441). These oligomers contained one double inter-flavan linkage (C-C and C-O-C bonds) which resulted in an additional loss of two H atoms (−2 Da) compared to the B-type molecules.

Several peaks exhibited multiple adduct ions from the same compound. With the exception of the common adducts formed under ESI positive ionization, such as [M+Na]$^+$, [2M+Na]$^+$, [M+NH$_4$]$^+$, and [M+H]$^+$, the extra [M+46]$^+$ adduct ions were observed for most peaks, and were determined as [M+C$_2$H$_8$N]$^+$ based on their accurate masses. These ions were identified as the adducts with ethylamine (CH$_3$CH$_2$NH$_2$), which was formed from the reduction of acetonitrile under ESI conditions [28]. Peak 1 with the molecular formula of $C_{19}H_{28}O_{13}$ had its main fragment ion at m/z 171 ($C_8H_{11}O_4$), suggesting a dimethoxy-hydroxyphenol group ($C_8H_{10}O_4$) in its structure. Based on its neutral loss of 294 Da (pentose and hexose), it was

putatively identified as "cinnacassoside C" (3,4-dimethoxy-5-hydroxyphenyl 6-O-apiofuranosylglucopyranoside), which has been previously identified in *C. cassia* [12]. Peak 3 with a formula of $C_{20}H_{30}O_{12}$ had its fragment ions at *m/z* 133, 151, and 265. The fragment ion at *m/z* 151 ($C_9H_{11}O_2$) and its dehydrated form (*m/z* 133, −18 Da) are consistent with a methoxy-ethylphenol structure, and the neutral loss of 312 Da (463→151) from the molecular ion suggests pentose and hexose moieties. The compound was putatively annotated as 3-methoxy-4-hydroxyphenylethyl 6-O-pentofuranosylhexopyranoside.

Peak 6 with a formula of $C_{19}H_{28}O_{12}$ had its main fragment ions at *m/z* 115, 155, 179, and 251. The ion at *m/z* 155 ($C_8H_{11}O_3$) corresponds to a dimethoxyphenol group ($C_8H_{10}O_3$) and the 294 Da neutral loss indicates pentose and hexose structures. Further comparison of its fragmentation pattern to the online mass spectral database mzCloud (HighChem LLC, Slovakia) revealed an excellent match with reference standard 3,4-dimethoxyphenyl 6-O-pentopyranosylhexopyranoside. A compound with the same structural formula was determined as 3,4-dimethoxyphenyl 6-O-apiofuranosylglucopyranoside in both *C. cassia* and other plant materials by HRMS and NMR [12, 29]. Therefore, peak 6 was tentatively identified as 3,4-dimethoxyphenyl 6-O-apiofuranosylglucopyranoside in the current study. Similarly, peak 12 with the molecular formula of $C_{20}H_{30}O_{12}$ and its major fragment ions at *m/z* 185 ($C_9H_{13}O_4$, trimethoxyphenol), 227, 281, and 317 was putatively annotated as 3,4,5-trimethoxyphenyl 6-O-apiofuranosylglucopyranoside after comparing its molecular formula and fragmentation pattern with the mzCloud mass spectral database (reference standard: 3,4,5-trimethoxyphenyl 6-O-pentopyranosylhexopyranoside). The same compound has been detected in *C. cassia* by different studies [12, 30].

Peak 13 with the formula of $C_{18}H_{26}O_{10}$ had main fragment ions at *m/z* 115, 133, 223, and 295. The fragment ion at *m/z* 295 is consistent with pentose and hexose moieties and the ion at *m/z* 133 ($C_5H_9O_4$) also corresponds to a pentose moiety. The neutral loss of 108 Da between the [M+H]$^+$ molecular ion and the *m/z* 295 fragment ion suggests a benzyl alcohol structure (C_7H_8O). Based on the sugar moiety types of the other identified components (i.e., peaks 1, 3, 6, and 12), it was putatively identified as benzyl 6-O-pentofuranosylhexopyranoside. Peak 16 has a formula of $C_{15}H_{20}O_8$ and fragment ions at *m/z* 121, 149, and 167. These fragments correspond to (hydroxyphenyl)propionic acid ($C_9H_{10}O_3$), its dehydrated form, and its fragment resulting from the loss of a carboxyl group (COOH). The neutral loss of 162 Da between the fragment at *m/z* 167 and the [M+H]$^+$ molecular ion suggests a hexose moiety. Based on this information, it was identified as dihydrocinnacasside (2-hydroxyphenylpropanoyl-O-glucopyranoside), which has been previously identified in *C. cassia* [16, 31]. Peak 17 ($C_{20}H_{28}O_{12}$) had main fragments at *m/z* 115, 133, and 167. The fragment at *m/z* 167 ($C_9H_{11}O_3$) is consistent with the ion structure of paeonol (2-hydroxy-4-methoxyphenylethanone) and the neutral loss of 294 Da from [M+H]$^+$ ion suggests hexose and pentose moieties. Other fragments at *m/z* 133 ($C_5H_9O_4$) and 115 ($C_5H_7O_3$) also suggests the structures of pentose and its dehydrated form. Thus, peak 17 was putatively identified as apiopaeonoside (paeonol-O-apiofuranosylglucopyranoside).

Peak 18 was determined to have formula of $C_{18}H_{16}O_4$ and fragments at *m/z* 237 ($C_{16}H_{13}O_2$) and 265 ($C_{17}H_{13}O_3$). The neutral loss of $C_2H_4O_2$ and CH_4O moieties suggests acetate and methoxy groups in its structure. Based on its formula, peak 18 was tentatively identified as

2-cinnamoyl-5-methoxyphenyl acetate. Peak 25 with a formula of $C_{26}H_{40}O_{12}$ had its main fragment ion at m/z 383 ($C_{20}H_{31}O_7$), which is consistent with the molecular ion of cinnacasol [13]. The neutral loss of 162 Da from the $[M+H]^+$ ion corresponds to a hexose moiety. It was tentatively annotated as cinnacaside (cinnacasol-glucoside), as the compound has been previously detected in *C. cassia* [13]. Peak 27 with its $[M+H]^+$ ion at m/z 183.0651 ($C_9H_{10}O_4$, –0.09 ppm) had fragment ions at m/z 95 and 123. The neutral loss of 60 Da ($C_2H_4O_2$, 183→123) suggests methyl (CH_3) and carboxylic (COOH) groups in its structure. It was tentatively identified as dimethoxybenzoic acid.

Peak 30 was determined to have the formula of $C_{20}H_{28}O_{10}$ and had a major fragment ion at m/z 117 (C_9H_9), which is consistent with the ion of dehydroxylated cinnamyl alcohol ($C_9H_{10}O$). The neutral loss of 312 Da suggests hexose and pentose moieties. It was putatively identified as rosavin (cinnamyl 6-O-arabinopyranosylglucopyranoside), which was primarily found in *Rhodiola rosea* [32] and has been reported in *C. cassia* as well [12]. Peak 32 with formula of $C_{22}H_{34}O_8$ had major fragments ions at m/z 331 ($C_{20}H_{27}O_4$), 349 ($C_{20}H_{29}O_5$), and 391 ($C_{22}H_{31}O_6$). These ions were resulted from the loss of H_2O and/or CH_2CO moieties. Such a fragmentation pattern aligns well with previous published data on cinnzeylanine, where fragments at m/z 347 and 329 were observed under negative ionization [33]. Cinnzeylanine as a diterpene acetate has been identified from different cinnamon species including *C. verum*, *C. loureiroi*, and *C. cassia* [33, 34].

Peak 33 ($C_9H_8O_2$) was identified as trans-cinnamic acid after comparing its LC and MS data with the authentic standard. Cinnamic acid is a common component in different cinnamon materials [15, 35]. Peak 34 with a formula of $C_{22}H_{26}O_8$ had major fragments at m/z 167 ($C_9H_{11}O_3$) and 330 ($C_{18}H_{18}O_6$). The neutral loss of the $C_4H_9O_2$ moiety ($C_{22}H_{26}O_8$→$C_{18}H_{18}O_6$) resulted from demethylation (–CH2) and demethoxylation (–CH3O) during ion fragmentation. Based on these data, peak 34 was putatively identified as syringaresinol, which has been detected in a traditional Chinese medicine containing the *C. cassia* twig [36].

3. Multivariate analyses of the metabolomic profiles of different cinnamon species

A simple comparison on the MS chromatograms in Fig. 1 reveals variations of certain cinnamon components among the 4 species. Most notably are coumarin (peak 31), which was substantially present in CM-1 (*C. burmannii*) and CM-6 (*C. loureiroi*); and methoxycinnamaldehyde (peak 35), which was barely detectable in CM-1 (*C. burmannii*) but was present at considerable concentrations in the other 3 species. For a comprehensive comparison of the metabolomic profiles of the different cinnamon species, multivariate analyses were conducted on the HRMS data of the analyzed cinnamon samples including PCA and PLS-DA that are unsupervised and supervised analyses, respectively.

Prior to the multivariate analyses, the MS data matrix was normalized to unit vector length. The normalization was applied to minimize the effects of certain factors on the consistency of sample analysis, including the nature of different cinnamon samples during manufacture (e.g. moisture level), MS ionization efficiency, LC sample injection consistency, and variability on sample preparation [37]. Fig. 2a and b are PCA and PLS-DA score plots. Cinnamon sample distributions were almost identical in the two analyses, and the 14

samples were clearly separated into four groups based on their species, which suggests that different cinnamon species can be discriminated by their metabolomic profiles. Although CM-5 contained DNA sequences of multiple cinnamon species from the DNA barcoding (Table 1), it was classified into the same group with the other *C. burmannii* samples (CM-1 to CM-4). CM-5 had the typical metabolomic profile of *C. burmannii* despite the ambiguous result from the DNA barcoding test. *C. loureiroi* and *C. cassia* samples, which cannot be discriminated by DNA barcoding, were well separated in both analyses. This separation further suggests the great potential of using metabolomics in cinnamon sample authentication and the occasional ambiguity of DNA barcoding. Similar results were reported in our lab's previous study on the differentiation of cinnamon species using the flow injection mass spectrometric (FIMS) fingerprinting method [20].

To determine important cinnamon metabolites contributing to the discrimination of different species, the variable loadings on the first two principal components (PCs) of PCA were plotted (Fig. 2c). Each "variable" in the MS data matrix refers to the MS chromatographic peak (cinnamon component) that was identified across different cinnamon samples. Variables with high loadings (absolute value) on PC1 and/or PC2 had a stronger influence on the corresponding component(s) and should exhibit larger variations among cinnamon species that were separated on the same component(s). For the PLS-DA analysis, the VIP scores of each variable were calculated and plotted (Fig. 2d) to represent their contributions to class (species) discrimination [38]. From the PCA loading plot, ten variables (1-10 in Fig. 2c) were selected to have high PCA loadings and significant variations among certain cinnamon species. Seven of these 10 variables also had high VIP scores (VIP score > 4) obtained from PLS-DA (Fig. 2d, Table 3), placing them at the top of the variable list contributing to the discrimination of cinnamon species. In fact, only one additional variable was determined to have a high VIP score (4.77) from PLS-DA but had moderate loadings from PCA (variable 11 in Fig. 2c).

The retention times and accurate mass data of each variable were used to determine their identities. Variable 2 with positive PC1 and PC2 scores was identified as cinnamaldehyde, which corresponds to peak 35 in Fig. 1 and Table 2. In Fig. 2a and b, *C. loureiroi* samples had high, positive PC1 and PC2 scores and *C. verum* samples had the lowest, negative scores. This result suggests that *C. loureiroi* contains high levels of cinnamaldehyde while *C. verum* does not. Indeed, in Fig. 3a, *C. loureiroi* samples had the highest ion abundance of cinnamaldehyde, significantly higher than the other species. On the other hand, *C. verum* samples exhibited the lowest level of cinnamaldehyde. Similar results were reported in previous studies which highlighted the high cinnamaldehyde content of *C. loureiroi* over other species [17, 39].

4. Identification of cinnamon species based on selected components

One of the main goals of this study was to identify cinnamon components that are differentially presented across species and can be used as chemical markers for cinnamon product differentiation or authentication. Considering the varied forms of cinnamon products and their different contents of cinnamon materials, using the absolute concentrations of marker components across different cinnamon products for identification purpose can be

inaccurate and misleading. The universal occurrence of cinnamaldehyde as the main, characteristic metabolite across different cinnamon species makes it an ideal reference compound for other components. Thus, for the rest of determined important cinnamon metabolites, the relative ion intensity with respect to the cinnamaldehyde intensity was calculated and compared among the different species. These results are given in Fig. 3b-f. In the figure, values labelled with different letters were significantly different under the Tukey HSD test ($p < 0.05$).

Variables 1 and 3 with negative PC1 loadings and positive PC2 loadings (Fig. 2c) were identified as methoxycinnamaldehyde and its fragment (Table 3). As a result, the *C. cassia* samples located in the same area of the PCA score plot (Fig. 2a, b) had the highest relative ion intensity of methoxycinnamaldehyde (against cinnamaldehyde) compared to the other species. Meanwhile *C. burmannii* samples located on the opposite side of the score plot had a much smaller methoxycinnamaldehyde relative ion intensity (Fig. 3b). These observations suggest methoxycinnamaldehyde can be used as a chemical marker to differentiate *C. burmannii* from other species. Moreover, cinnamaldehyde and its methoxylated form were proposed as the most potent bioactive components contributing to cinnamon's anti-inflammatory properties [9]. Thus, the above data suggest that *C. cassia* and *C. loureiroi* could carry more anti-inflammatory benefits than the other two species.

Variable 10 with both the highest VIP score (15.01) and variable loading on PC1 (0.74) was identified as coumarin (peak 31 in Fig. 1 and Table 2). In Fig. 2a and b, *C. loureiroi* and *C. burmannii* samples had high, positive PC1 scores and *C. verum* samples had the lowest, negative scores. This result suggests that *C. loureiroi* and *C. burmannii* should contain high levels of coumarin while *C. verum* contains lower levels. In Fig. 3c, the relative ion abundance of coumarin was significantly higher in *C. burmannii* and *C. loureiroi* samples, while for *C. verum* the coumarin peak only had a minute relative ion intensity. These data are consistent with a previous study on the coumarin contents of different cinnamon species [17]. As a result, coumarin can be applied as the chemical marker to (1) discriminate *C. verum* from other cinnamon species, especially *C. burmannii* and *C. loureiroi*; and (2) differentiate *C. loureiroi* and *C. cassia* samples as most of the other components failed to show significant variation between the two species. The potential hepatotoxic and carcinogenic effects of coumarin have drawn concerns on its safety as food ingredient [40, 41]. Thus, the use of *C. verum* cinnamon species as a food ingredient would not be a significant source of dietary coumarin and the use of the other species should be regulated.

Variables 4, 5, and 6 located on the left, bottom part of the loading plot (Fig. 2c), the same as *C. verum* samples in the score plot (Fig. 2a, b). Variable 5 was identified as 2-cinnamoyl-5-methoxyphenyl acetate and variables 4 and 6 were putatively characterized as alkaloids with formulas of $C_{19}H_{23}NO_3$ and $C_{19}H_{23}NO_4$, respectively. These three compounds, especially 2-cinnamoyl-5-methoxyphenyl acetate, were primarily produced in *C. verum* samples compared to others (Fig. 3d-f). They can be added in the list of chemical markers differentiating *C. verum* from other cinnamon species.

Other variables (variable 7-9, 11) were identified as A-type or B-type PACs (Table 3). While the three A-type PACs (variables 7-9) located at the bottom of loading plot with negative

PC2 loadings, variable 11 is the only B-type PAC (DP-2) that had a positive PC2 loading (Fig. 2c). This finding suggests that A-type and B-type PACs were differentially produced among the four cinnamon species. To validate this assumption, ion abundances of monomers, A-type, and B-type PACs were compared across the 4 cinnamon species. In Fig. 4a, *C. burmannii* samples contained significantly more PACs than the other species, and A-type molecules accounted for 80% of the total ion intensity. Similarly, *C. verum* samples also had A-type PACs (70%) as the major components. In contrast, *C. cassia* and *C. loureiroi* samples mainly produced B-type molecules, which accounted for over 90% (97% for *C. loureiroi*) of their total PACs. As a result, the ratio of A-type versus B-type PACs was 4.1 for *C. burmannii* and 2.4 for *C. verum* and reduced to 0.01 and 0.03 for *C. loureiroi* and *C. cassia*, respectively (Fig. 4b).

Similar results for the relative abundance of A-type versus B-type PACs in different cinnamon species were observed in our previous analysis using the FIMS fingerprinting method [20]. In the current study, the use of UHPLC–HRMS allowed us to specifically determine the ratios of different PAC subgroups (monomer, A-type, and B-type) in cinnamon samples and compare them across different species. Although several existing studies have reported the structure of PAC molecules in specific cinnamon species (e.g., A-type PACs in *C. verum* or *C. burmannii*; B-type PACs in *C. cassia*) [11, 14, 42], to our knowledge, this report is the first comparing the composition of PAC subgroups of the major cinnamon species. Our results suggest the potential of using PAC composition to differentiate certain cinnamon species. Because PACs also occur in other botanicals (e.g., cranberry and cocoa), it should be noted that this method would only apply to samples with cinnamon as the sole source of PACs.

Cinnamon PACs appeared to be the major active components contributing to many of the spice's health benefits, such as antidiabetic effect, antibacterial activity, and antioxidant property [7, 8, 11, 42]. A-type and B-type PACs, differing by their inter-flavan linkage types, exhibit different levels of bioactivities such as anti-adhesion property against bacteria, inhibitory effects on pancreatic lipase, and antioxidant activity [43-45]. In cinnamons, a study has also reported that different cinnamon extracts rich in A-type or B-type PACs acted under different mechanisms for their hypoglycemic effects [42]. Our data suggests that the source (species) of cinnamon material can be decisive for their bioactivities, thus it would be necessary to conduct preliminary analysis on the chemical composition of cinnamon materials prior to their bioactivity evaluation. For health benefits related to the overall or A-type PACs, *C. burmannii* should be considered as the best source. For bioactivities due to B-type PACs, *C. cassia* appeared to be the better choice over other species.

The proposed steps for differentiating the four cinnamon species is shown on Fig. 5. First, *C. loureiroi* and *C. cassia* can be easily differentiated from *C. burmannii* and *C. verum* using ratios and A-type against B-type PACs as *C. loureiroi* and *C. cassia* contain mostly B-type PACs, and *C. burmannii* and *C. verum* contain mostly A-type PACs (Fig. 4). Next, coumarin/cinnamaldehyde ratios can be used to differentiate *C. loureiroi* from *C. cassia* as the former has a significantly higher ratio compared to *C. cassia* (Fig. 3c). Lastly, differentiation of *C. burmannii* and *C. verum* can also be achieved using coumarin/cinnamaldehyde ratio as *C. burmannii* has a significantly higher ratio compared to *C. verum* (Fig. 3c). This result can be

further confirmed by 2-cinnamoyl-5-methoxyphenyl acetate/cinnamaldehyde ratio as *C. verum* has a significantly higher ratio than the other species (Fig. 3d).

The major testing methods and acceptance criteria of two USP monographs for identification of *C. cassia* and *C. verum* barks are summarized in Electronic Supplementary Material (ESM) Table S1 [46, 47]. The acceptance criteria for cinnamaldehyde and total phenolic contents are partially overlapped between the two species, which leaves cinnamic acid and coumarin as the only two available components for species differentiation. Compared to these methods, our strategy proposed above shows several distinctive advantages. First, so far only two cinnamon species are associated with monographs while all four major cinnamon species are included in the proposed strategy. Second, quantitative analyses using HPLC, Folin-Ciocalteu Assay, or GC are need in monographs to determine contents of specific components, which can be time consuming and require authentic reference standards. In our method, only semi-quantitative data from MS analysis are needed for proper identification. Third, the current monographs are limited as they can only be applied to pure cinnamon samples and may not able to identify cinnamon in complex matrices, such as cinnamon dietary supplements as the analytical methods in the monographs lack the necessary specificity needed. In contrast, since the proposed method in the current study uses relative contents of certain cinnamon components comparing to cinnamaldehyde, it can be potentially applied in complex materials containing cinnamons such as dietary supplements.

To further evaluate the efficacy of selected metabolites (Table 3) in cinnamon species differentiation, their ion abundances were extracted from the original MS data matrix to form a second data set with a size of 11 variables. Both sets of spectra were transformed by taking the cubic roots of the ion abundances and normalizing to unit vector length. The cubic root transformation inflates the effect of small values in the data matrix on chemometric modeling, and was shown to outperform other data transformation methods (e.g., logarithmic and other root transformations) on the classification of cannabis cultivars using MS data with chemometrics [48]. The support vector tree classifier was constructed using each set and the average prediction accuracies were compared. With 2 Latin partitions and 100 bootstraps, both data sets had excellent prediction accuracies of 100%. This result indicates that there was no loss of information by only selecting the 11 metabolites in the data set when performing cinnamon sample classification. It further validates our proposed strategy for identification of cinnamon species using specific metabolites as chemical markers.

Conclusions

Cinnamon is one of the most widely used spices and continues to receive growing interest for a variety of health benefits. We comprehensively characterized the metabolomic profiles of four major cinnamon species - *C. burmannii*, *C. loureiroi*, *C. cassia*, and *C. verum*, using UHPLC–HRMS. Thirty-six metabolites were identified that belong to various compound groups. PCA and PLS-DA analyses on the HRMS metabolomic data matrix identified several key cinnamon metabolites that can be used as chemical markers for cinnamon sample authentication and differentiation. This study further expands the current knowledge

on cinnamon phytochemical composition and highlights the metabolomic variation of major cinnamon species. Data presented in the study will offer valuable insights on evaluating the health benefit potentials of selected cinnamon materials and support future studies focusing on the action mechanisms of cinnamons' various bioactivities.

Supplementary Material

Refer to Web version on PubMed Central for supplementary material.

Acknowledgements:

References

1. Gruenwald J, Freder J, Armbruester N. Cinnamon and health. Crit Rev Food Sci Nutr. 2010;50:822–34. [PubMed: 20924865]

2. Bandara T, Uluwaduge I, Jansz ER. Bioactivity of cinnamon with special emphasis on diabetes mellitus: A review. Int J Food Sci Nutr. 2012;63:380–6. [PubMed: 22007625]

3. Ravindran PN, Babu KN, Shylaja M. Cinnamon and Cassia: The genus Cinnamonum. CRC Press; 2004.

4. Leung AY. Encyclopedia of common natural ingredients used in food, drugs, and cosmetics. Wiley; 1980.

5. Toriizuka K Basic lecture of Kampo medicine: pharmacological effect of cinnamon. Kampo Med. 1998;11:431–6.

6. Medagama AB, Bandara R. The use of Complementary and Alternative Medicines (CAMs) in the treatment of diabetes mellitus: is continued use safe and effective? Nutr J. 2014;13:102. [PubMed: 25331834]

7. Shan B, Cai YZ, Brooks JD, Corke H. Antibacterial properties and major bioactive components of cinnamon stick (*Cinnamomum burmannii*): Activity against foodborne pathogenic bacteria. J Agric Food Chem. 2007;55:5484–90. [PubMed: 17567030]

8. Tulini FL, Souza VB, Thomazini M, Silva MP, Massarioli AP, Alencar SM, Pallone EMJA, Genovese MI, Favaro-Trindade CS. Evaluation of the release profile, stability and antioxidant activity of a proanthocyanidin-rich cinnamon (*Cinnamomum zeylanicum*) extract co-encapsulated with α-tocopherol by spray chilling. Food Res Int. 2017;95:117–24. [PubMed: 28395819]

9. Gunawardena D, Karunaweera N, Lee S, Van Der Kooy F, Harman DG, Raju R, Bennett L, Gyengesi E, Sucher NJ, Münch G. Anti-inflammatory activity of cinnamon (*C. zeylanicum* and *C. cassia*) extracts - Identification of E-cinnamaldehyde and o-methoxy cinnamaldehyde as the most potent bioactive compounds. Food Funct. 2015;6:910–9. [PubMed: 25629927]

10. Bernard D, Kwabena A, Osei O, Daniel G, Elom S, Sandra A. The Effect of Different Drying Methods on the Phytochemicals and Radical Scavenging Activity of Ceylon Cinnamon (*Cinnamomum zeylanicum*) Plant Parts. European J Med Plants. 2014;4:1324–35.

11. Anderson RA, Broadhurst CL, Polansky MM, Schmidt WF, Khan A, Flanagan VP, Schoene NW, Graves DJ. Isolation and Characterization of Polyphenol Type-A Polymers from Cinnamon with Insulin-like Biological Activity. J Agric Food Chem. 2004;52:65–70. [PubMed: 14709014]

12. Luo Q, Wang SM, Lu Q, Luo J, Cheng YX. Identification of compounds from the water soluble extract of *Cinnamomum cassia* barks and their inhibitory effects against high-glucose-induced mesangial cells. Molecules. 2013;18:10930–43. [PubMed: 24013407]

13. Tran MN, Do TH, Lee IS, Min BS, Na MK, Jung HJ, Lee SM, Bae KH. Two new diterpenes from the twigs of *Cinnamomum cassia*. Helv Chim Acta. 2009;92:2058–62.

14. Nonaka G, Morimoto S, Nishioka I. Tannins and related compounds. Part 13. Isolation and structures of trimeric, tetrameric, and pentameric proanthicyanidins from cinnamon. J Chem Soc Perkin Trans 1. 1983;2139–45.

15. Ho SC, Chang KS, Chang PW. Inhibition of neuroinflammation by cinnamon and its main components. Food Chem. 2013;138:2275–82. [PubMed: 23497886]

16. Ngoc TM, Lee I, Ha DT, Kim H, Min B, Bae K. Tyrosinase-Inhibitory Constituents from the Twigs of *Cinnamomum cassia*. J Nat Prod. 2009;72:1205–8. [PubMed: 19555125]

17. Wang YH, Avula B, Nanayakkara NPD, Zhao J, Khan IA. Cassia cinnamon as a source of coumarin in cinnamon-flavored food and food supplements in the United States. J Agric Food Chem. 2013;61:4470–6. [PubMed: 23627682]

18. Wijesekera RO. Historical overview of the cinnamon industry. CRC Crit Rev Food Sci Nutr. 1978;10:1–30. [PubMed: 363362]

19. Avula B, Smillie TJ, Wang Y-H, Zweigenbaum J, Khan IA. Authentication of true cinnamon (*Cinnamon verum*) utilising direct analysis in real time (DART)-QToF-MS. Food Addit Contam Part A. 2015;32:1–8.

20. Chen P, Sun J, Ford P. Differentiation of the four major species of cinnamons (*C. burmannii, C. verum, C. cassia*, and *C. loureiroi*) using a flow injection mass spectrometric (FIMS) fingerprinting method. J Agric Food Chem. 2014;62:2516–21. [PubMed: 24628250]

21. Oketch-Rabah HA, Marles RJ, Brinckmann JA. Cinnamon and cassia nomenclature confusion: a challenge to the applicability of clinical data. Clin Pharmacol Ther. 2018;104:435–45. [PubMed: 29947417]

22. Harrington PB. Support vector machine classification trees based on fuzzy entropy of classification. Anal Chim Acta. 2017;954:14–21. [PubMed: 28081808]

23. Harrington PB. Multiple versus single set validation of multivariate models to avoid mistakes. Crit Rev Anal Chem. 2018;48:33–46. [PubMed: 28777019]

24. Harrington PB. Statistical validation of classification and calibration models using bootstrapped Latin partitions. TrAC -Trends Anal Chem. 2006;25:1112–24.

25. Schymanski EL, Jeon J, Guide R, Fenner K, Ruff M, Singer HP, Hollender J. Identifying small molecules via high resolution mass spectrometry: communicating confidence. Environ Sci Technol. 2014;48:2097–8. [PubMed: 24476540]

26. Friedrich W, Eberhardt A, Galensa R. Investigation of proanthocyanidins by HPLC with electrospray ionization mass spectrometry. Eur Food Res Technol. 2000;211:56–64.

27. Lin LZ, Harnly JM. Quantitation of flavanols, proanthocyanidins, isoflavones, flavanones, dihydrochalcones, stilbenes, benzoic acid derivatives using ultraviolet absorbance after identification by liquid chromatography-mass spectrometry. J Agric Food Chem. 2012;60:5832–40. [PubMed: 22577798]

28. Gu ZM, Ma J, Zhao XG, Wu J, Zhang D. Reduction of nitriles to amines in positive ion electrospray ionization mass spectrometry. Rapid Commun Mass Spectrom. 2006;20:2969–72. [PubMed: 16952212]

29. Jiang J, Feng Z, Wang Y, Zhang P. New Phenolics from the Roots of Symplocos caudata WALL. Chem Pharm Bull. 2005;53:110–3. [PubMed: 15635243]

30. Shiraga Y, Okano K, Akira T, Fukaya C, Yokoyama K, Tanaka S, Fukui H, Tabata M. Structures of potent antiulcerogenic compounds from *Cinnamomum cassia*. Tetrahedron. 1988;44:4703–11.

31. Kim SY, Koo YK, Koo JY, Ngoc TM, Kang SS, Bae K, Kim YS, Yun-Choi HS. Platelet anti-aggregation activities of compounds from *Cinnamomum cassia*. J Med Food. 2010;13:1069–74. [PubMed: 20828311]

32. Tolonen A, Pakonen M, Hohtola A, Jalonen J. Phenylpropanoid glycosides from *Rhodiola rosea*. Chem Pharm Bull. 2003;51:467–70. [PubMed: 12673010]

33. Tanaka K, Li F, Tezuka Y, Watanabe S, Kawahara N, Kida H. Evaluation of the quality of Chinese and Vietnamese cassia using LC-MS and multivariate analysis. Nat Prod Commun. 2013;8:75–8. [PubMed: 23472464]

34. Isogai A, Suzuki A, Tamura S, Ohashi Y, Sasada Y. Cinnzeylanine, a new pentacyclic diterpene acetate from *Cinnamonum zeylanicum*. Acta Crystallogr Sect B Struct Crystallogr Cryst Chem. 1977;33:623–6.

35. Ding Y, Wu EQ, Liang C, Chen J, Tran MN, Hong CH, Jang Y, Park KL, Bae K, Kim YH, Kang JS. Discrimination of cinnamon bark and cinnamon twig samples sourced from various countries using HPLC-based fingerprint analysis. Food Chem. 2011;127:755–60. [PubMed: 23140731]

36. Li M, Hung A, Li H, Yang AW. A classic herbal formula Guizhi Fuling Wan for menopausal hot flushes: from experimental findings to clinical applications. Biomedicines. 2019;7:60.

37. Alfassi ZB. On the normalization of a mass spectrum for comparison of two spectra. J Am Soc Mass Spectrom. 2004;15:385–7. [PubMed: 14998540]

38. Farrés M, Platikanov S, Tsakovski S, Tauler R. Comparison of the variable importance in projection (VIP) and of the selectivity ratio (SR) methods for variable selection and interpretation. J Chemom. 2015;29:528–36.

39. Li YQ, Kong DX, Wu H. Analysis and evaluation of essential oil components of cinnamon barks using GC-MS and FTIR spectroscopy. Ind Crops Prod. 2013;41:269–78.

40. Abraham K, Wöhrlin F, Lindtner O, Heinemeyer G, Lampen A. Toxicology and risk assessment of coumarin: Focus on human data. Mol Nutr Food Res. 2010;54:228–39. [PubMed: 20024932]

41. Lake BG. Coumarin metabolism, toxicity and carcinogenicity: Relevance for human risk assessment. Food Chem Toxicol. 1999;37:423–53. [PubMed: 10418958]

42. Chen L, Sun P, Wang T, Chen K, Jia Q, Wang H, Li Y. Diverse mechanisms of antidiabetic effects of the different procyanidin oligomer types of two different cinnamon species on db/db mice. J Agric Food Chem. 2012;60:9144–50. [PubMed: 22920511]

43. Dong XQ, Zou B, Zhang Y, Ge ZZ, Du J, Li CM. Preparation of A-type proanthocyanidin dimers from peanut skins and persimmon pulp and comparison of the antioxidant activity of A-type and B-type dimers. Fitoterapia. 2013;91:128–39. [PubMed: 24001713]

44. Kimura H, Ogawa S, Akihiro T, Yokota K. Structural analysis of A-type or B-type highly polymeric proanthocyanidins by thiolytic degradation and the implication in their inhibitory effects on pancreatic lipase. J Chromatogr A. 2011;1218:7704–12. [PubMed: 21803362]

45. Howell AB, Reed JD, Krueger CG, Winterbottom R, Cunningham DG, Leahy M. A-type cranberry proanthocyanidins and uropathogenic bacterial anti-adhesion activity. Phytochemistry. 2005;66:2281–91. [PubMed: 16055161]

46. United States Pharmacopeia. In-Process Revision: *Cinnamomum cassia* bark. Pharmacopeial Forum 40(5).

47. United States Pharmacopeia. In-Process Revision: *Cinnamomum verum* bark. Pharmacopeial Forum 40(5).

48. Dong W, Liang J, Barnett I, Kline PC, Altman E, Zhang M. The classification of Cannabis hemp cultivars by thermal desorption direct analysis in real time mass spectrometry (TD-DART-MS) with chemometrics. Anal Bioanal Chem. 2019;411:8133–42. [PubMed: 31776640]
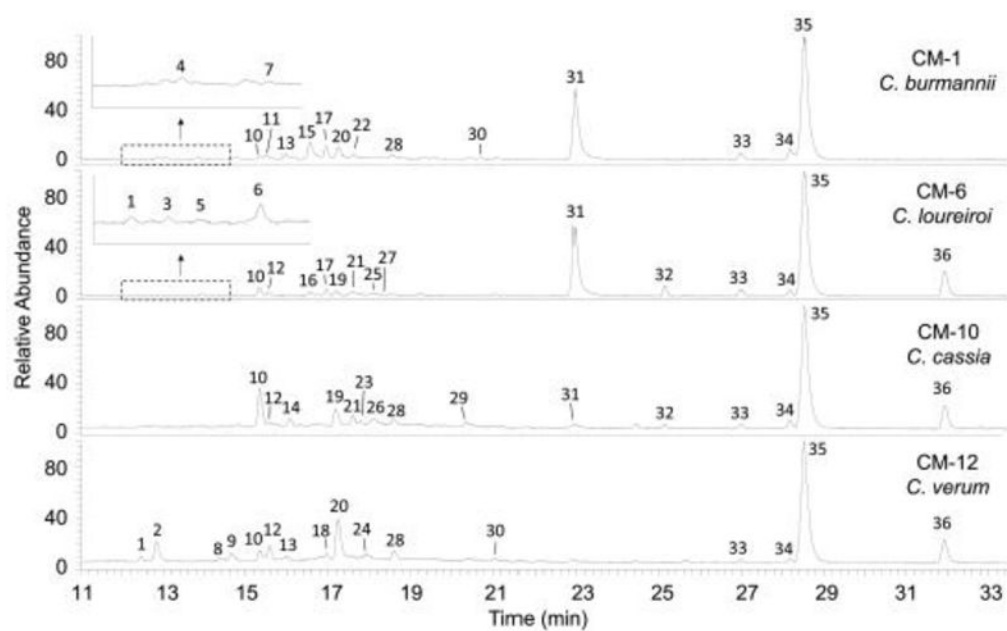
Fig. 1.
Total ion chromatograms (TIC) of selected cinnamon extracts. Peak labels correspond to numbers in Table 2
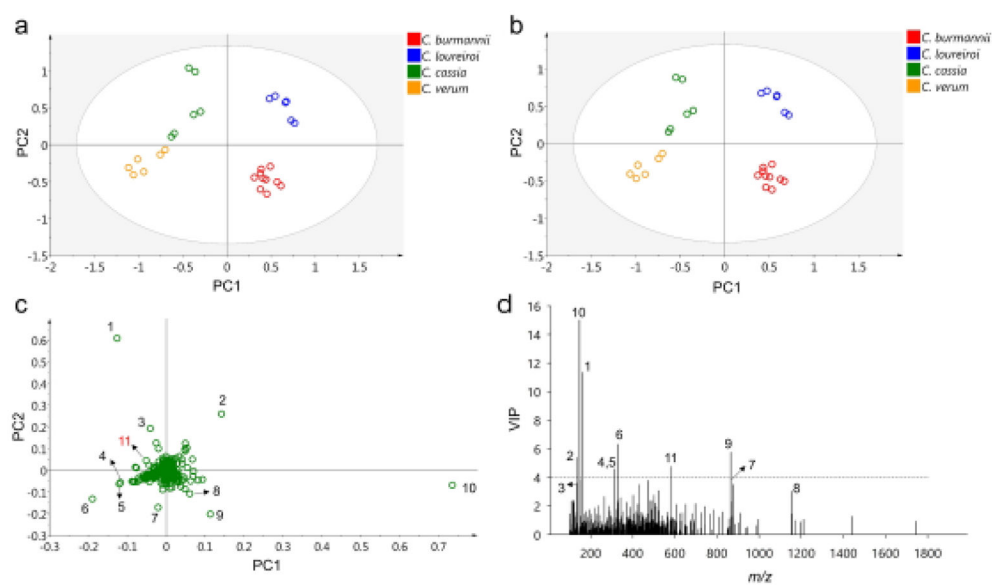
Fig. 2.
PCA and PLS-DA analyses on the metabolomic profiles of different cinnamon species. a: PCA score plot; b: PLS-DA score plot; c: PCA loading plot. Variable labels correspond to numbers in Table 3; d: Variable importance in the projection (VIP) score plot of PLS-DA. Variable labels correspond to numbers in Table 3
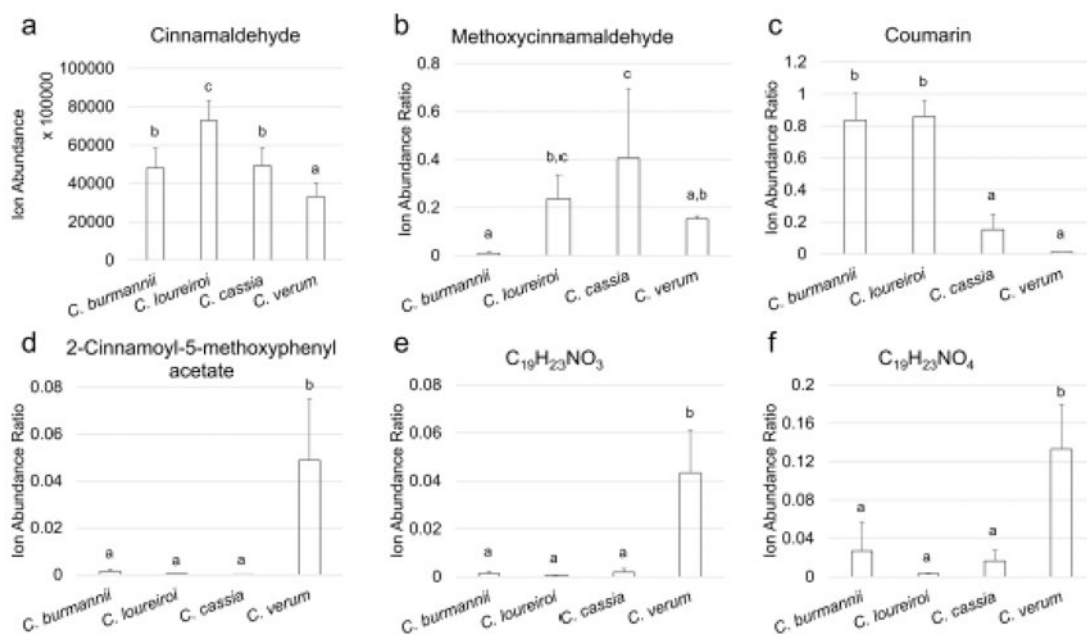
Fig. 3.
Levels of important metabolites in four cinnamon species. Metabolites were determined by PCA and PLS-DA. a: average ion abundance of cinnamaldehyde; b-f: relative ion abundance ratio of other metabolites against cinnamaldehyde. In each chart, value bars labeled with different letters have significant difference ($p < 0.05$)
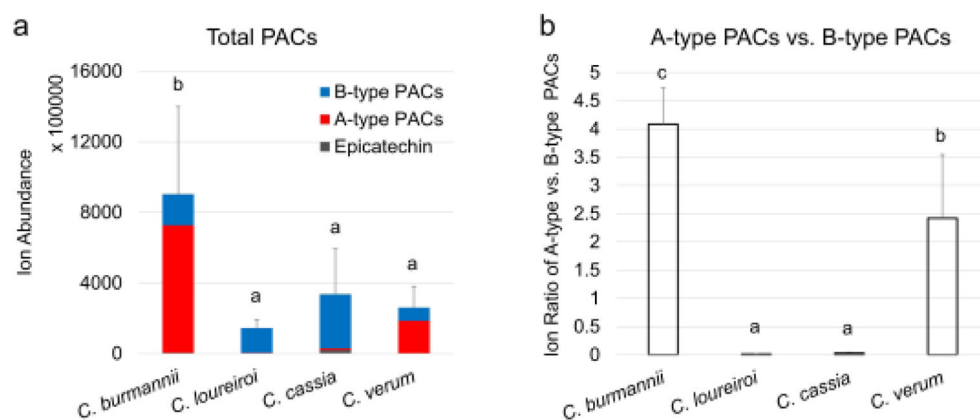
Fig. 4.

Proanthocyanidin compositions in four cinnamon species. a: total ion abundance of identified PACs; b: Ratio of A-type against B-type PACs. In each chart, values bars labeled with different letters have significant difference ($p < 0.05$)
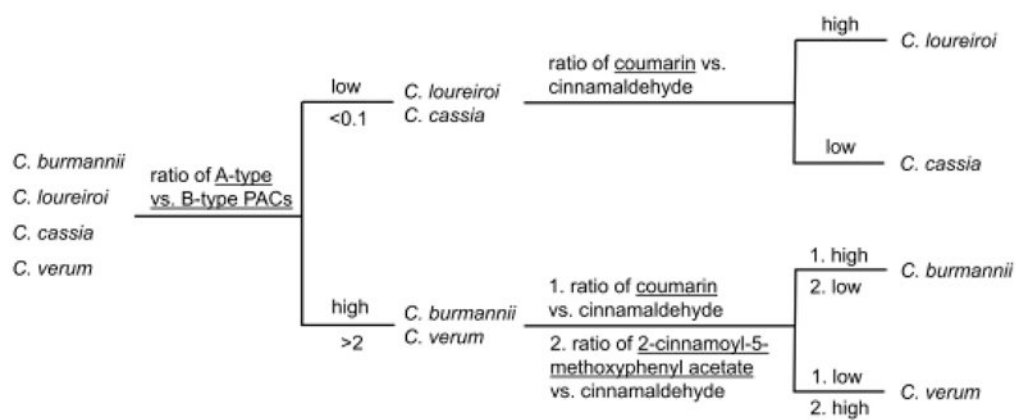
Fig. 5.
Differentiation of four cinnamon species by their ratios of specific marker components
determined by LC-MS

Table 1.

Authentication of analyzed cinnamon products using DNA barcoding.

Sample code	Product description	[a]Origin	Form	DNA barcoding result - *Species* (No. of sequences)	[b]Determined species
CM-1	Korintje Cinnamon Powder, Certified Organic, *Cinnamomum burmannii*	NA	powder	*C. burmannii*	*C. burmannii*
CM-2	Cinnamon Powder Organic, *Cinnamomum burmannii*	Indonesia	powder	*C. burmannii* (2245)	*C. burmannii*
CM-3	Indonesian "Korintje" Cassia Cinnamon	NA	stick	*C. burmannii* (2892), *C. loureiroi* or *C. cassia* (91)	*C. burmannii*
CM-4	Cassia Bark Korintje Cinnamon	NA	chip	*C. burmannii* (6846), *C. loureiroi* or *C. cassia* (25), other plants (79)	*C. burmannii*
CM-5	Organic Korintje Cinnamon	Indonesia	powder	*C. burmannii* (571), *C. loureiroi* or *C. cassia* (1808)	ND
CM-6	Organic Vietnamese Cinnamon	NA	powder	*C. loureiroi* or *C. cassia* (3985)	*C. loureiroi*
CM-7	Saigon Cinnamon	NA	powder	*C. loureiroi* or *C. cassia* (1138), *C. burmannii* (42)	*C. loureiroi*
CM-8	Saigon Cinnamon Sticks	NA	stick	*C. loureiroi* or *C. cassia* (528)	*C. loureiroi*
CM-9	Cassia Bark	China	chip	*C. loureiroi* or *C. cassia* (3697)	*C. cassia*
CM-10	Chinese Cinnamon Bark	NA	chip	*C. loureiroi* or *C. cassia* (6457), other plants (3015)	*C. cassia*
CM-11	Chinese Cinnamon	NA	powder	*C. loureiroi* or *C. cassia* (4645), other plants (182)	*C. cassia*
CM-12	Ceylon Cinnamon	Sri Lanka	stick	*C. verum* (3569), other plants (4)	*C. verum*
CM-13	Ceylon Cinnamon Powder, Certified Organic, *Cinnamomum verum*	NA	powder	*C. verum* (5305), other plants (3013)	*C. verum*
CM-14	Organic Ceylon Cinnamon Powder	Sri Lanka	powder	*C. verum* (3402), other plants (306)	*C. verum*

[a]NA: not available

[b]ND: not determined

Table 2.

UHPLC–HRMS data of cinnamon metabolites.

Peak	Rt (min)	m/z	Adduct type	Formula	Error (ppm)	Major fragment ions	[a]Tentative identification
1	12.44	510.2186	[M+C$_2$H$_7$N +H]$^+$	C$_{19}$H$_{28}$O$_{13}$	0.95	510→171.0650(100). 267.0864(76)	Cinnacassoside C
		487.1427	[M+Na]$^+$		1.0		
		465.1605	[M+H]$^+$		0.5		
2	12.85	1153.2607	[M+H]$^+$	C$_{60}$H$_{48}$O$_{24}$	-0.07	247.0605(33), 287.0549(100), 695.5070(24)	A-type PAC DP-4 (A=1)
3	12.86	508.2491	[M+C$_2$H$_7$N +H]$^+$	C$_{20}$H$_{30}$O$_{12}$	0.49	508→133.0645(62), 151.0751(48), 265.1069(100)	3-Methoxy-4-hydroxyphenylethyl 6-O-pentofuranosylhexopyranoside
		485.1633	[M+Na]$^+$		0.73		
		463.1812	[M+H]$^+$		0.43		
4	13.05	579.1498	[M+H]$^+$	C$_{30}$H$_{26}$O$_{12}$	0.34	127.0386(96), 289.0706(100), 291.0862(88)	B-type PAC DP-2
5	13.24	579.1498	[M+H]$^+$	C$_{30}$H$_{26}$O$_{12}$	0.34	127.0388(100), 289.0708(82), 291.0865(82)	B-type PAC DP-2
6	13.91	494.2236	[M+C$_2$H$_7$N +H]$^+$	C$_{19}$H$_{28}$O$_{12}$	0.81	466→115.0387(75), 155.0700(100), 179.0700(94), 251.0912(90)	3,4-Dimethoxyphenyl 6-O-apiofuranosylglucopyranoside
		471.1477	[M+Na]$^+$		0.86		
		466.1922	[M+NH$_4$]$^+$		0.64		
7	14.04	1153.2607	[M+H]$^+$	C$_{60}$H$_{48}$O$_{24}$	−0.07	247.0595(56), 287.0549(100), 664.3065(30), 766.9262(30)	A-type PAC DP-4 (A=1)
8	14.37	1441.3245	[M+H]$^+$	C$_{75}$H$_{60}$O$_{30}$	0.28	1441→287.0547(100), 672.6395(80),1031.6045(63), 1201.3632(69)	A-type PAC DP-5 (A=1)
		721.1664	[M+2H]$^{2+}$		0.65		
9	14.64	1441.3237	[M+H]$^+$	C$_{75}$H4$_{60}$O$_{30}$	−0.52	1441→247.0591(53), 287.0543(100), 289.0692(27)	A-type PAC DP-5 (A=1)
		721.1662	[M+2H]$^{2+}$		0.45		
10	15.31	579.1500	[M+H]$^+$	C$_{30}$H$_{26}$O$_{12}$	0.45	127.0387(97), 289.0705(74), 291.0861(100)	B-type PAC DP-2
11	15.43	1153.2600	[M+H]$^+$	C$_{60}$H$_{48}$O$_{24}$	−0.71	247.0595(42), 287.0549(100), 289.0710(33)	A-type PAC DP-4 (A=1)
12	15.55	524.2340	[M+C$_2$H$_7$N +H]$^+$	C$_{20}$H$_{30}$O$_{13}$	0.45	496→185.0807(100), 227.0914(24), 281.1021(28), 317.1232(13)	3,4,5-Trimethoxyphenyl 6-O-apiofuranosylglucopyranoside
		501.1583	[M+Na]$^+$		0.87		
		496.2029	[M+NH$_4$]$^+$		0.87		
		479.1758	[M+H]$^+$		−0.12		
13	15.96	827.2940	[2M+Na]$^+$	C$_{18}$H$_{26}$O$_{10}$	−0.50	420→115.0387(100), 133.0493(85), 223.0964(29), 295.1023(17)	Benzyl 6-O-pentofuranosylhexopyranoside
		448.2177	[M+C$_2$H$_7$N +H]$^+$		−0.05		

Peak	Rt (min)	m/z	Adduct type	Formula	Error (ppm)	Major fragment ions	[a]Tentative identification
		425.1420	[M+Na]+		0.43		
		420.1866	[M+NH$_4$]+		0.18		
14	16.06	291.0866	[M+H]+	$C_{15}H_{14}O_6$	−0.22	123.0440(51), 139.0389(100), 165.0547(26)	[b]Epicatechin
15	16.53	865.1976	[M+H]+	$C_{45}H_{36}O_{18}$	0.16	287.0549(100), 301.0716(24), 533.1079(21), 575.1190(4)	A-type PAC DP-3 (A=1)
16	16.57	374.1815	[M+C$_2$H$_7$N +H]+	$C_{15}H_{20}O_8$	1.5	346→121.0646(8), 149.0595(67), 167.0702(100)	Dihydrocinnacasside
		351.1054	[M+Na]+		1.0		
		346.1501	[M+NH$_4$]+		0.46		
17	16.93	506.2238	[M+C$_2$H$_7$N +H]+	$C_{20}H_{28}O_{12}$	1.2	478→115.0389(34), 133.0495(29), 167.0702(100)	Apiopaeonoside
		483.1479	[M+Na]+		1.2		
		478.1925	[M+NH$_4$]+		0.60		
18	16.96	314.1388	[M+NH$_4$]+	$C_{18}H_{16}O_4$	0.37	297→237.0909(24), 265.0860(100)	2-Cinnamoyl-5-methoxyphenyl acetate
		297.1123	[M+H]+		0.16		
19	17.18	867.2129	[M+H]+	$C_{45}H_{38}O_{18}$	−0.19	127.0388(80), 289.0706(100), 291.0863(60), 579.1486(26)	B-type PAC DP-3
20	17.23	865.1973	[M+H]+	$C_{45}H_{36}O_{18}$	−0.14	287.0548(100), 301.0711(32), 533.1029(28)	A-type PAC DP-3 (A=1)
21	17.60	1155.2771	[M+H]+	$C_{60}H_{50}O_{24}$	0.62	276.1558(100), 289.0701(85), 291.0869(100)	B-type PAC DP-4
22	17.62	328.1544	[M+H]+	$C_{19}H_{21}NO_4$	0.07	265.0857(52), 297.1119(100)	Unknown alkaloid
23	17.79	1443.3407	[M+H]+	$C_{75}H_{62}O_{30}$	0.83	146.2928(100), 1138.4525(52)	B-type PAC DP-5
24	17.95	1153.2607	[M+H]+	$C_{60}H_{48}O_{24}$	−0.13	339.2633(97), 507.2888(94), 739.7498(100), 864.5703(97)	A-type PAC DP-4 (A=1)
25	18.06	590.3176	[M+C$_2$H$_7$N +H]+	$C_{26}H_{40}O_{12}$	0.84	590→383.2064(100)	Cinnacaside
		567.2418	[M+Na]+		1.1		
		545.2598	[M+H]+		0.55		
26	18.12	1443.3405	[M+H]+	$C_{75}H_{62}O_{30}$	0.63	173.4246(100), 1342.9332(76)	B-type PAC DP-5
27	18.51	183.0651	[M+H]+	$C_9H_{10}O_4$	−0.09	95.0491(62), 123.0440(100)	Dimethoxybenzoic acid
28	18.56	330.1701	[M+H]+	$C_{19}H_{23}NO_4$	0.35	192.1019(100)	Unknown alkaloid
29	20.33	579.1502	[M+H]+	$C_{30}H_{26}O_{12}$	0.50	127.0387(87), 289.0707(83), 291.0864(100)	B-type PAC DP-2

Peak	Rt (min)	m/z	Adduct type	Formula	Error (ppm)	Major fragment ions	[a]Tentative identification
30	21.07	879.3253	[2M+Na]$^+$	$C_{20}H_{28}O_{10}$	−0.47	446→117.0697(100)	Rosavin
		474.2236	[M+C$_2$H$_7$N+H]$^+$		0.48		
		451.1577	[M+Na]$^+$		0.51		
		446.2022	[M+NH$_4$]$^+$		0.13		
31	22.96	147.0439	[M+H]$^+$	$C_9H_6O_2$	−0.16	91.0541(29), 103.0540(100)	Coumarin
32	25.08	875.4411	[2M+Na]$^+$	$C_{22}H_{34}O_8$	1.3	444→331.1904(100), 349.2014(76), 391.2127(66)	Cinnzeylanine
		472.2912	[M+C$_2$H$_7$N+H]$^+$		1.5		
		449.2152	[M+Na]$^+$		0.61		
		444.2598	[M+NH$_4$]$^+$		1.4		
33	26.98	149.0598	[M+H]$^+$	$C_9H_8O_2$	0.63	103.0540(26), 131.0489(100)	[b]Trans-cinnamic acid
34	28.15	859.3147	[2M+Na]$^+$	$C_{22}H_{26}O_8$	−0.06	401→167.0703(100), 330.1099(93)	Syringaresinol
		401.1598	[M-H$_2$O+H]$^+$		0.80		
35	28.49	133.0646	[M+H]$^+$	C_9H_8O	−0.19	55.0178(100), 105.0697(31), 115.0541(88)	Cinnamaldehyde
36	31.94	163.0755	[M+H]$^+$	$C_{10}H_{10}O_2$	0.14	55.0178(100), 107.0490(95), 135.0804(96)	Methoxycinnamaldehyde

[a]PAC: proanthocyanidin; DP: degree-of-poplymerization; A: No. of A-type linkage

[b]Compound structures were confirmed by authentic standards

Table 3.

Important cinnamon metabolites determined by PCA and PLS-DA on different cinnamon species.

No.	Variable ID (Rt_*m/z*)	PCA loadings		[a]VIP score (PLS-DA)	Identity (peak No. in Table 2)
		PC1	PC2		
1	31.93_163.0755	−0.13	0.61	11.35	Methoxycinnamaldehyde (36)
2	28.51_133.0647	0.14	0.26	5.40	Cinnamaldehyde (35)
3	31.93_135.0804	−0.04	0.19	3.60	Methoxycinnamaldehyde fragment (35)
4	15.50_314.1754	−0.12	−0.06	4.30	Alkaloid, $C_{19}H_{23}NO_3$
5	16.95_314.1391	−0.12	−0.06	4.60	2-Cinnamoyl-5-methoxyphenyl acetate (18)
6	18.60_330.1703	−0.19	−0.13	6.32	Alkaloid, $C_{19}H_{23}NO_4$ (28)
7	17.24_865.1982	−0.02	−0.17	3.91	A-type PAC DP-3 (A=1) (20)
8	15.44_1153.2606	0.06	−0.11	3.03	A-type PAC DP-4 (A=1) (11)
9	16.52_865.1979	0.11	−0.20	5.77	A-type PAC DP-3 (A=1) (15)
10	22.95_147.0440	0.74	−0.07	15.01	Coumarin (31)
11	15.32_579.1503	−0.05	0.04	4.77	B-type PAC DP-2 (10)

[a]VIP: variable importance in the projection